



## Supplementary Material

# Effect of Cu Intercalation Layer on the Enhancement of Spin-to-Charge Conversion in Py/Cu/Bi<sub>2</sub>Se<sub>3</sub>

Shu Hsuan Su <sup>1,\*</sup>, Cheong-Wei Chong <sup>1</sup>, Jung-Chuan Lee <sup>1,6</sup>, Yi-Chun Chen <sup>1</sup>,  
Vyacheslav Viktorovich Marchenkov <sup>2,3</sup> and Jung-Chun Andrew Huang <sup>1,4,5,\*</sup>

<sup>1</sup> Department of Physics, National Cheng Kung University, Tainan 701401, Taiwan

<sup>2</sup> M.N. Miheev Institute of Metal Physics, UB RAS, Ekaterinburg 620108, Russia

<sup>3</sup> Institute of Physics and Technology Ural Federal University, Ekaterinburg 620002, Russia

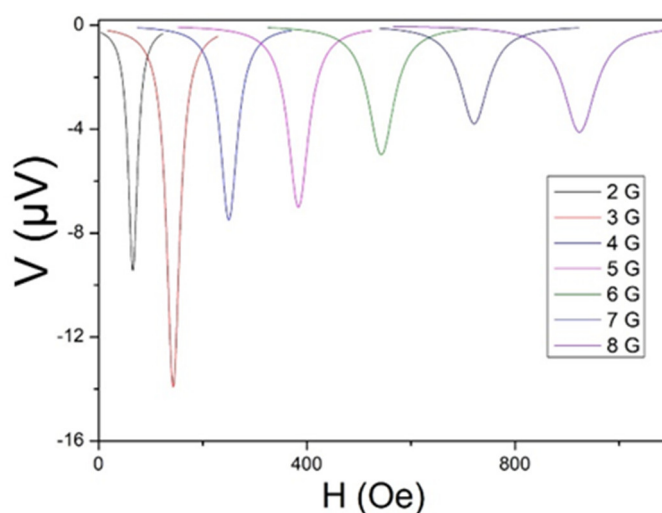
<sup>4</sup> Department of Applied Physics, National University of Kaohsiung, Kaohsiung 811726, Taiwan

<sup>5</sup> Taiwan Consortium of Emergent Crystalline Materials, National Science and Technology Council, Taipei 10622, Taiwan

<sup>6</sup> Sheng Chuang Technology Company, Taichung 407330, Taiwan

\* Correspondence: macg0510@yahoo.com.tw (S.H.S.); jcahuang@mail.ncku.edu.tw (J.-C.A.H.)

## Section 1. The spin pumping voltage for various excitation frequencies and magnetic field scans



**Citation:** Su, S.H.; Chong, C.-W.; Lee, J.-C.; Chen, Y.-C.; Marchenkov, V.V.; Huang, J.-C.A. Effect of Cu Intercalation Layer on the Enhancement of Spin-to-Charge Conversion in Py/Cu/Bi<sub>2</sub>Se<sub>3</sub>. *Nanomaterials* **2022**, *12*, 3687. <https://doi.org/10.3390/nano12203687>

Academic Editor: Ze Don Kvon

Received: 17 September 2022

Accepted: 17 October 2022

Published: 20 October 2022

**Publisher's Note:** MDPI stays neutral with regard to jurisdictional claims in published maps and institutional affiliations.



**Copyright:** © 2022 by the authors. Licensee MDPI, Basel, Switzerland. This article is an open access article distributed under the terms and conditions of the Creative Commons Attribution (CC BY) license (<https://creativecommons.org/licenses/by/4.0/>).

**Figure S1.** Spin pumping induced voltage in Py/Cu(7nm)/Bi<sub>2</sub>Se<sub>3</sub> measured at various excitation frequencies. The obtained  $V$  decreases with the increase of frequency, which is resulted from variation of the performance of the microwave transmission line at different frequencies.

**Figure S2.** shows spin pumping voltage obtained by sweeping the magnetic-field ( $H$ ), measured in the Py/Bi<sub>2</sub>Se<sub>3</sub> sample for three in-plane field direction given by  $\varnothing = 0^\circ, 90^\circ$  and  $180^\circ$ , as illustrated in the inset. As expected from the  $V \propto J_s \times \sigma(\sigma$  is the direction of spin polarization,  $\sigma \parallel H$ ), the  $V$  values are maximum for  $\varnothing = 0^\circ$  and  $180^\circ$  and  $V$  value almost vanishes as  $\varnothing = 90^\circ$ . When magnetic field was reversed ( $\varnothing = 0^\circ$  and  $180^\circ$ ), the observed spin pumping signal changed sign as expected from the IEE, indicating that the spin accumulation is reversed on the edge on changing the direction of the magnetic field. It further provides evidence of the IEE induced from spin-momentum locked surface state in Bi<sub>2</sub>Se<sub>3</sub>.

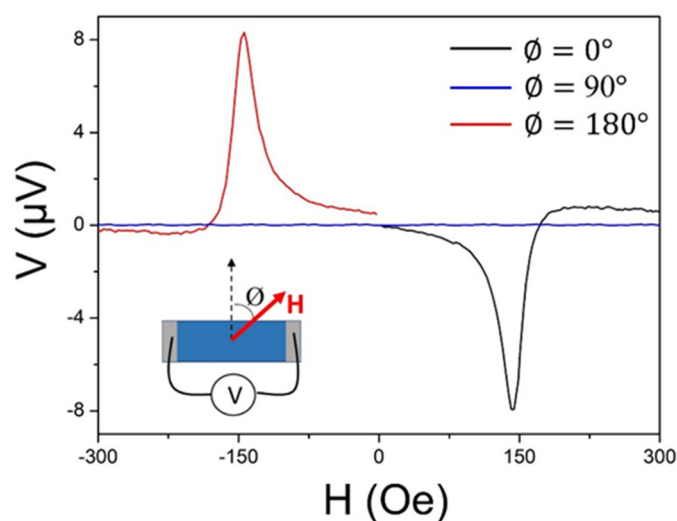


**Figure S2.** Magnetic field scans of the spin pumping voltage measured in Py/Bi<sub>2</sub>Se<sub>3</sub> at three different in-plane angles as illustrated in the inset.

## Section 2. The structural characterization of Bi<sub>2</sub>Se<sub>3</sub> thin films and Py/Cu/ Bi<sub>2</sub>Se<sub>3</sub> trilayer

The structural characterization of Bi<sub>2</sub>Se<sub>3</sub> thin films was performed by X-ray diffraction (XRD) and atomic force microscopy (AFM). Fig. S3(a) shows the X-ray  $\theta$ -2 $\theta$  scans of the samples. Several features collinear with the direction (00l) were observed, indicating that the single crystal films were grown along the c-axis direction. Large-area surfaces of Bi<sub>2</sub>Se<sub>3</sub> films were observed with AFM measurement (in Fig. S3(b)). Large and flat terraces and straight steps are the characteristics of high-quality Bi<sub>2</sub>Se<sub>3</sub> film. The triangular shape of the islands is consistent with the lattice symmetry of Bi<sub>2</sub>Se<sub>3</sub> (0001) surface. [1, 2] The measured line profile of the height in Fig. S3(d) (corresponding to the red line in Fig. S3(b)) shows that the step height is 1.0 nm, corresponding to the quintuple layer (QL) of Bi<sub>2</sub>Se<sub>3</sub> structure. [2, 3] The reflection high-energy electron diffraction (RHEED) shows sharp streaky 1 $\times$ 1 pattern, indicating high quality of the Bi<sub>2</sub>Se<sub>3</sub> (0001) surface (inset of Fig. S3(b)), which corresponds well to the AFM data. We also applied high-resolution transmission electron microscopy (HRTEM) to examine the quality of Py/Cu/ Bi<sub>2</sub>Se<sub>3</sub> trilayer. Fig. S3(c) shows the HRTEM image along the c axis, clearly showing the epitaxial growth of the Bi<sub>2</sub>Se<sub>3</sub> film. It can be seen that the interface is flat and continuous, which is important for effective spin pumping.

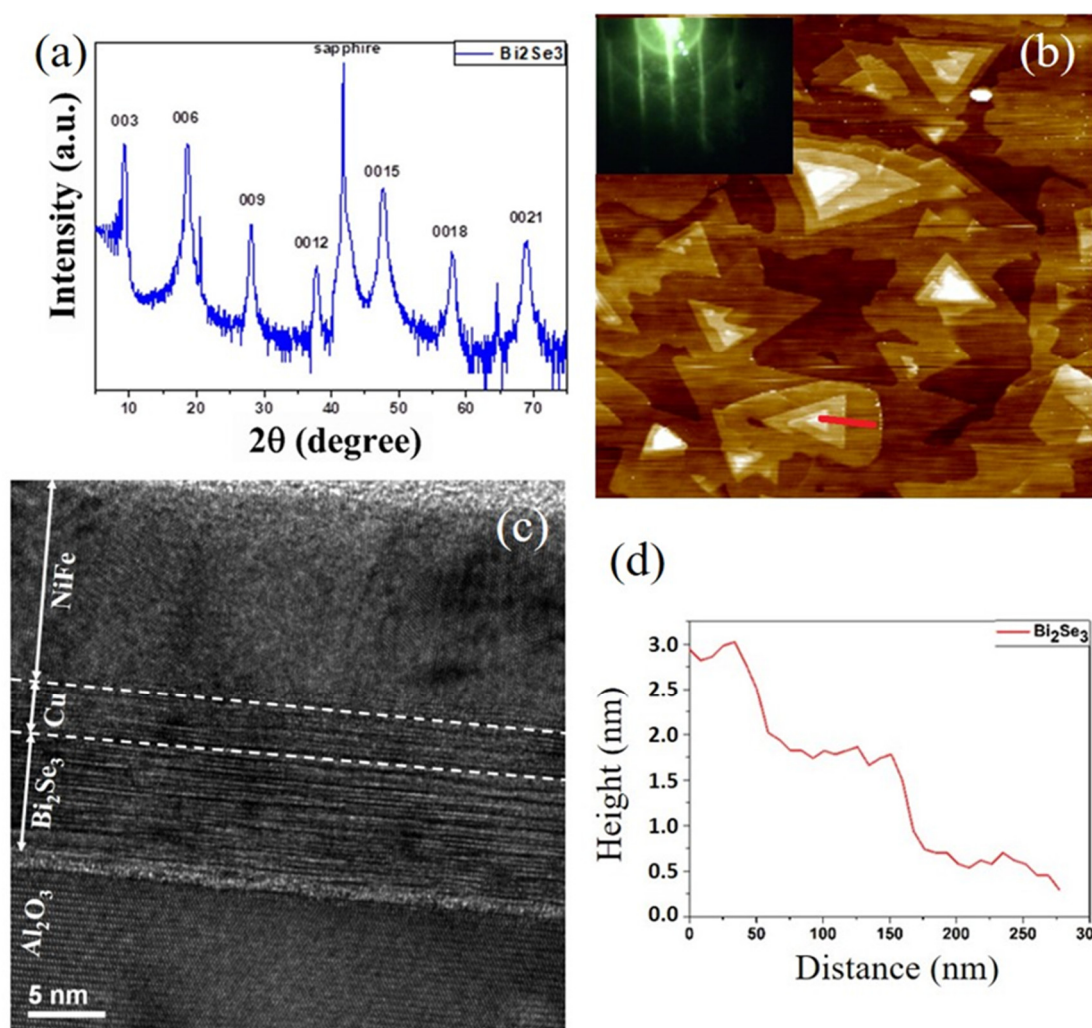


**Figure S3.** The structure of  $\text{Bi}_2\text{Se}_3$  film. (a) XRD pattern of  $\text{Bi}_2\text{Se}_3$  film on  $c$ -plane sapphire substrate (b) AFM image of  $10\text{QL Bi}_2\text{Se}_3$  film (scale:  $2\ \mu\text{m} \times 2\ \mu\text{m}$ ). The inset shows the corresponding RHEED pattern. (c) TEM cross-sectional image of a  $\text{Py/Cu} (\sim 3\ \text{nm})/\text{Bi}_2\text{Se}_3$  sample. (d) Line scan profile corresponding to the red line in (b).

#### Reference:

1. Cheng, P.; Song, C.; Zhang, T.; Zhang, Y.; Wang, Y.; Jia, J.-F.; Wang, J.; Wang, Y.; Zhu, B.-F.; Chen, X.; Ma, X.; He, K.; Wang, L.; Dai, X.; Fang, Z.; Xie, X.; Qi, X.-L.; Liu, C.-X.; Zhang, S.-C.; & Xue, Q.-K. Landau Quantization of Topological Surface States in  $\text{Bi}_2\text{Se}_3$ . *Phys. Rev. Lett.* **2010**, *105*, 076801.
2. Su, S.H.; Chuang, P.-Y.; Chen, S.W.; Chen, H.Y.; Tung, Y.; Chen, W.-C.; Wang, C.-H.; Yang, Y.-W.; Huang, J.C.A.; Chang, T.-R.; et al. Selective Hydrogen etching leads to 2D  $\text{Bi}(111)$  bilayers on  $\text{Bi}_2\text{Se}_3$ : Large Rashba splitting in topological insulator heterostructure. *Chem. Mater.* **2017**, *29*, 8992–9000.
3. Atuchin, V. V.; Golyashov, V. A.; Kokh, K. A.; Korolkov, I. V.; Kozhukhov, A. S.; Kruchinin, V. N.; Makarenko, S. V.; Pokrovsky, L. D.; Prosvirin, I. P.; Romanyuk, K. N.; Tereshchenko, O. E. Formation of Inert  $\text{Bi}_2\text{Se}_3(0001)$  Cleaved Surface. *Cryst. Growth Des.* **2011**, *11*, 5507–5514.